[4], ($1.658 \times 10^{-11}y^{-1} \pm 1.6\%$) [6]. All these studies gave consistent results with about 2× better uncertainty than the direct determination [5]. It is necessary to note that all these results contain an additional source of uncertainty that is difficult to estimate, the "link" between the object dated with the Re-Os method and the one used as a reference point with a well-determined absolute age. Smoliar et al. [3] ascribed the angrite Pb-Pb age to their IIIA isochron on the basis of Cr-Mn data for angrites and IIIAB irons. Shukolyukov and Lugmair [6] ascribed the angrite Pb-Pb age to IIA irons assuming the same Re-Os age for IIA irons and pallasites and demonstrated the same Cr-Mn formation interval for pallasites and angrites. Shen et al. [4] ascribed the oldest Pb-Pb age for Allende inclusions to their IIA isochron.

A better way for refining the decay constant is Re-Os dating of an object that has been precisely dated using a long-lived isotope system. The IAB iron meteorite group gives the best opportunity for such a comparison since silicate inclusions that are abundant in IAB meteorites have numerous age determinations (e.g., Rb-Sr [7], K-Ar [8], Sm-Nd [9]).

Rhenium-osmium results for studied IA samples are presented in Fig. 1. The data define a precise isochron with a slope uncertainty of 0.5%. With the Re decay constant $1.666 \times 10^{-11}y^{-1}$ [3], this isochron yields an age of 4529 ± 23 Ma, in very good agreement with the Sm-Nd result of [9] (4.52 ± 0.02 Ga). The statistical analysis of the slope uncertainties of these isochrons indicates that this ^{187}Re decay constant is consistent with the accepted Sm decay constant within 0.6%.

Acknowledgments: This work was partially supported by Sigma Xi student research grant.

References: [1] Creaser R. A. et al. (1991) *GCA, 55,* 397. [2] Shirey S. B. and Walker R. J. (1995) *Anal. Chem., 34,* 2136. [3] Smoliar M. I. et al. (1996) *Science, 271,* 1099. [4] Shen J. J. et al. (1996) *GCA, 60,* 2887. [5] Linder M. et al. (1989) *GCA, 53,* 1597. [6] Shukolyukov A. and Lugmair G. W. (1997). [7] Burnett D. S. and Wasserburg G. J. (1967) *EPSL, 2,* 397. [8] Bogard D. et al. (1967) *EPSL, 3,* 275. [9] Stewart B. et al. (1996) *EPSL, 143,* 1.

THE ENVIRONMENT AND GEOLOGICAL SETTING OF THE SOUTH POLE OF THE MOON FROM CLEMENTINE DATA. P. D. Spudis, D. B. J. Bussey, and K. R. Stockstill, Lunar and Planetary Institute, 3600 Bay Area Boulevard, Houston TX 77058, USA (spudis@lpi.jsc.nasa.gov).

The Clementine mission mapped the Moon globally in 1994, including giving us our first detailed look at the lunar south polar region. The south pole lies within the rim crest of the 2500-km-diameter South Pole-Aitken (SPA) Basin, the largest recognized impact feature on the terrestrial planets. In addition, the pole lies within cratered terrain, where the average relief exceeds 3–5 km on scales of tens of kilometers. Because the Moon's spin axis is inclined only 1.6° from the ecliptic, the Sun always appears at the horizon near the lunar poles and the amount of relief found in these areas suggests that certain zones may be in permanent sunlight or permanent darkness. We have made a new Clementine image mosaic of the south polar region using the latest edition of the lunar global control network to better study the lighting conditions and, by inference, the local topographic environment of the south polar area. Results confirm previous findings that about 16,000 km² of permanent darkness exist within ~200 km (7°) of the pole. Moreover, we have found several areas, each a few kilometers in size, that appear to be solar illuminated for longer periods of time than half of the 708-hr lunar day. The presence of large dark areas near the southern pole is in contrast to the situation at the north pole. In this region, no large basin that overlaps the polar area is present. In consequence, only the very small region near the crater Peary A (at the north pole, ~20 km in diameter) appears to be in permanent darkness (only about 300 km²). Thus, although ice may have accumulated near the northern pole of the Moon over geological time, the extent of the northern cold trap is much less than that of the cold traps in the southern polar area. The Clementine bistatic radar experiment was designed to use radio waves to look for coherent backscatter opposition effect (CBOE), a characteristic of ice-rich planetary surface targets (e.g., surface of Europa and Ganymede, polar caps of Mars, dark regions near the poles of Mercury). Data were collected from four orbits, two over each pole, and CBOE was observed on only one orbit, whose $\beta = 0$ groundtrack fell over the permanently dark areas near the south pole. This finding indicates the presence of ice on the Moon, a conclusion supported by observations of radar backscatter near the pole from Arecibo Observatory. The strength of the CBOE result (1 dB signal increase in RCP/LCP) is consistent with an average concentration level of ~0.3–0.5 wt% H_2O, integrated over the radar footprint. This corresponds to an equivalent volume of about 1 km³ of H_2O or 1 billion mT. The south pole of the Moon is an ideal site to explore and, ultimately, inhabit. Polar sites have an interesting and complex geological target: the floor of SPA Basin, which may have stripped off the crust and exposed the lunar mantle. From here, we can conduct astronomical observations of the entire southern sky, including using the Earth-blocked farside for radio-quiet observations of the sky. The local resources, in particular abundant H_2O ice (for life support and propellant production) and near-permanent sunlight of selected areas [for solar power and to take advantage of the benign thermal environment (average temperature is constantly about −30° ± 10°C)], greatly facilitate operations on the Moon and in Earth-Moon space.

PRECURSORS OF ALUMINUM-RICH CHONDRULES FROM THE AXTELL (CV3) METEORITE. G. Srinivasan, G. R. Huss, and G. J. Wasserburg, Division of Geological and Planetary Sciences, California Institute of Technology, Pasadena CA 91125, USA.

Aluminum-rich chondrules are less refractory and have lower ^{26}Al abundance compared to Ca-Al-rich inclusions (CAIs) [1–3]. The presence of hibonite grains in a Sharps Al-rich chondrule [2], and of a spinel-fassaite fragment in an Allende ferromagnesian chondrule [4] suggest CAIs as plausible precursors of Al-rich chondrules. To investigate this possibility we have determined major,-minor-, and rare-earth-element (REE) concentration in dominant mineral phases in CAIs and Al-rich chondrules from Axtell. Aluminum-rich chondrules from Axtell have $(^{26}Al/^{27}Al)_i \leq 3 \times 10^{-6}$ [1]. Bulk compositions for the chondrules were calculated from modal mineral abundances.

The type A AXCAI2771 has a group II pattern [5] with LREE ~75× CI chondrite. AXCAI1571 (type A) has nearly flat and ~10× CI-enriched REE pattern, with positive Eu and Yb anomalies. In the type B AXCAI2775 the bulk REE composition increases from 10× CI for LREE to 100× CI for HREE, with a negative anomaly in Yb. The REE composition of Axtell CAIs are consistent with those observed in Allende CAIs [e.g., 5].

AXCH1471 consists of intergrown laths of anorthitic plagioclase ($An_{>95}$) and (Ti-rich) aluminous diopside. Small spinel grains including spinel pallisade bodies and large olivines are also present. AXCH1471 has an ~10× CI-enriched REE pattern with a minor relative depletion of LREE. AXCH1371 has a mineralogy and texture similar to AXCH1471 and has a few partially resorbed spinel grains. AXCH1371 is 5–10× CI enriched in REE and refractory lithophiles and has small positive Eu, Tm, and Yb anomalies. AXCH2171 has a barred olivine texture with an intergrowth of pyroxene and plagioclase, and is ~10× CI enriched in REE and refractory lithophiles.

The lower REE enrichments and less-refractory bulk compositions of Al-rich chondrules suggest that Al-rich chondrules could be mixtures of CAIs and less-fractionated nebular material. The partially resorbed spinel in AXCH1371 and other textural features may be remnants of CAI fragments incorporated into the chondrule precursors and remelted. To test this hypothesis, mixing calculations were performed using several generic CAI compositions [5] and the CI composition as the less-fractionated component. The calculations assume that (1) generic CAI REE enrichment =20× CI with a flat pattern and (2) the product has Al_2O_3 = 22%. The mixing proportions for CI matrix and CAIs of type B1, B2, and fine grained are ~20–30% and ~70–80% respectively and for type A CAI and CI matrix it is 55% and 45% respectively.

Our calculations give compositions that agree within ~20% for AXCH1471 for Si, Ca, Mg, Ti, Cr, and HREE (LREE are too high in the calculation because we used a flat CAI REE pattern). Volatile elements (Na, K, Mn) and Fe and Ni are too high in our calculated compositions by factors of >2. The volatiles were perhaps lost from the chondrule during the chondrule-forming event or during thermal processing of its precursor. During

chondrule formation Fe and Ni were possibly expelled as metallic globules [e.g., 10]. The match between the calculated compositions and that of AXCH2171 is almost as good as for AXCH1471, except at Ti, which is much lower in the chondrule. None of our calculated compositions produced a good match with AXCH1371. Our calculations suggest that some Al-rich chondrules in Axtell may be products of mixing between CAI-like material and less fractionated nebular material, but others certainly are not. The mixing proportions show that low $^{26}Al/^{27}Al$ values in Al-rich chondrules cannot be explained by dilution due to mixing, but require a time delay of a few million years.

Acknowledgments: Work supported by NASA grant NAGW-3297. Div. Contrib. #5826(972).

References: [1] Srinivasan G. et al. (1996) *Meteoritics & Planet. Sci., 31*, A133. [2] Bischoff A. and Keil K. (1984) *GCA, 48*, 693–709. [3] Russell S. S. et al. (1996) *Science, 273*, 757–762. [4] Misawa K. and Fujita T. (1994) *Nature, 368*, 723–726. [5] MacPherson G. J. et al. (1988) in *Meteorites and Early SolarSystem* (J. F. Kerridge and M. S. Matthews, eds.), pp. 746–807, Arizona Univ. [6] Sheng Y. J. et al. (1991) *GCA, 55*, 581–599. [10] Connolly H. C. Jr. et al. (1994) *Nature, 371*, 136–139.

PROLONGED IRIDIUM DEPOSITION AFTER THE CRETACEOUS-TERTIARY BOUNDARY: THE PRIMARY SIGNAL FROM AN IMPACT-GENERATED TEMPORARY RING AROUND THE EARTH?

M. Stage[1] and K. L. Rasmussen[2], [1]Geological Survey of Denmark and Greenland, Thoravej 8, DK-2400 Copenhagen, Denmark (stage@gandalf.natmus.min.dk), [2]Carbon-14 Dating Laboratory, National Museum, Ny Vestergade 11, DK-1471 Copenhagen, Denmark.

The Ir distribution with depth at the Cretaceous-Tertiary boundary worldwide exhibits shoulders stratigraphically up and down from the high-Ir layer. The shoulders have been interpreted as a secondary signal from bioturbation and/or diffusion [1,2]. Although the Ir distributions do not have exactly the same shape globally, they exhibit the same general features. In the Cretaceous they gradually increase toward the boundary, followed by a maximum at the basal boundary layer. The rate of increase is fast and might seem exponential, as expected from diffusion processes. The decrease in the Ir enrichment in the Tertiary is prolonged (i.e., a wider distribution) and does not resemble an exponential decrease expected for a diffusional process. Instead the decrease is more noisy. We interpret the Ir distribution shoulder after the boundary as a primary accretion signal from a temporary planetary ring around the Earth, created by a major impact (i.e., the formation of the Chicxulub crater).

We have constructed a new three-dimensional computer model, simulating the orbital decay due to atmospheric drag of impact ejecta inserted into Keplerian orbits around the Earth. The typical size of the ejecta particles is estimated to be 0.4 mm in diameter, adopted from Melosh [3], who estimates the size of condensing droplets from a vaporized ejecta after a terrestrial impact with a 10-km impactor. We have monitored the number of interparticle collisions in such a ring. The particles experience very few collisions in their lifetime, thus collisions are omitted from our present model. With the model we estimate the lifetime of a dilute planetary ring around the Earth, and construct accretion profiles, depicting the amount of accreting material as a function of time.

Figure 1 shows the particles mean residence time in the ring as a function of the initial mean distance to the center of the Earth. The particles stay in the ring thousands of years at the shown heights. A timespan of thousands of years is in good agreement with Hansen et al. [4], who reported a deposition time for the Ir of 10–40,000 yr. The deposition time was estimated from Milankovitch cycles in the magnetic susceptibility signal across the K/T boundary.

Figure 2 shows the number of particles accreted onto the Earth as a function of time, calculated by our model. The accretion of ring material will start after the impact that created the maximum Ir concentration. A large fraction of the ring material will accrete just after the impact, followed by a slow decrease in the amount of accreting ring particles. In this situation the accretion ends after ~18,000 yr. This scenario will, in the sediment, be reflected as a maximum concentration of Ir at the boundary, followed by a shoulder of the Ir peak.

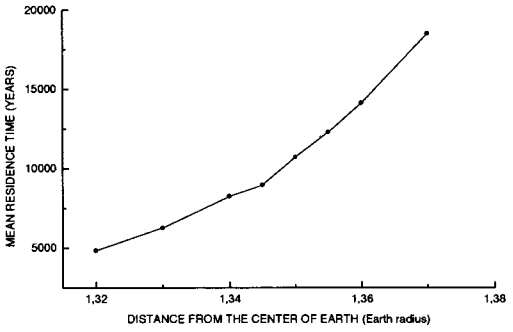

Fig. 1. The mean residence time for the particles in the ring increases for increasing initial distance to the Earth.

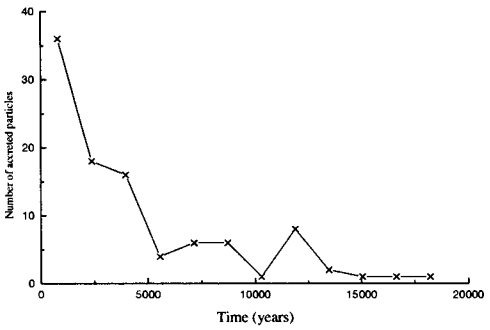

Fig. 2. Accretion distribution of the ring particles resembling the Tertiary shoulder of the Ir distribution.

Thus we hypothesize that debris from a more or less oblique impact was injected into the atmosphere, constituting a very dilute ring around the Earth for thousands of years. The ring material slowly accretes onto the Earth in thousands of years after the impact, prolonging the Ir enrichment into the Tertiary. The impact itself creates the Ir maximum together with the other well-known impact features described, such as Ni-rich spinels, shocked quartz and the Chicxulub impact crater.

References: [1] Robin D. et al. (1991) *LPS XXII*, 1125–1126. [2] Alvarez W. et al. (1990) *Science, 250*, 1700–1702. [3] Melosh H. J. (1989) in *Impact Cratering: A Geologic Process*, Oxford Univ. [4] Hansen H. J. et al. (1992) *Meteoritics, 27*, 230.

TIME-OF-FLIGHT SECONDARY ION MASS SPECTROMETRY (TOF-SIMS) ANALYSIS OF THE ORGUEIL CI METEORITE AT HIGH LATERAL RESOLUTION.

T. Stephan[1], D. Rost[1], E. K. Jessberger[1], and W. Klöck[2], [1]Institut für Planetologie, Wilhelm-Klemm-Strasse 10, D-48149 Münster, Germany (stephan@nwz.uni-muenster.de), [2]Institut für Geologische Wissenschaften, Domstrasse 5, D-06108 Halle, Germany.

Besides some interplanetary dust particles, CI meteorites represent, chemically, the most pristine solar system material available so far for laboratory investigation. Except for H, C, N, O, and the noble gases their composition is representative for the entire solar system [1]. Nevertheless, only little is known about the actual distribution of minor and trace elements in CI chondrites. Especially for the understanding of the apparent enrichments of volatile trace elements observed in interplanetary dust [2], the knowledge of their distribution in chondritic matter is important. Imaging time-of-flight secondary ion mass spectrometry (TOF-SIMS) at high lateral resolution seems to be an appropriate technique to analyze the element distribution within CI meteorites. On the other hand, an investigation of the Orgueil